ZANCO Journal of Pure and Applied Sciences

TYPE Original article
DOI http://dx.doi.org/10.21271/ZJPAS.38.2.4

Evaluation of Binary and Ternary Deep Eutectic Solvents as Sustainable High-Performance Base Lubricants

Ranj Suhail Khurshid*, Essa Ismaeil Ahmed

Department of chemistry, college of education, Salahaddin University-Erbil, Erbil, Kurdistan Region, Iraq

OPEN ACCESS

*Corresponding author

Ranj Suhail Khurshid

ranj.khurshid@su.edu.krd

RECEIVED :08 /07 /2025
ACCEPTED :05/10/ 2025
PUBLISHED: 30/04/2026

KEYWORDS:

Binary and ternary DESs, Tafel plots, Tribology, Corrosion resistance, ChCl, Mineral base oils.

ABSTRACT

The development of high-performance, environmentally friendly lubricants is crucial for sustainable industrial practices. This study investigates the synthesis and comprehensive characterization of binary and novel ternary deep eutectic solvents (DESs) made from choline chloride (ChCl) with various hydrogen bond donors (HBDs): urea, glycerol (Gly), ethylene glycol (EG), and oxalic acid (OA). Fourier-transform infrared FT-IR spectroscopy confirmed the formation of stable hydrogen-bonded networks in all DES formulations. Detailed analysis of their physicochemical, tribological, and electrochemical properties revealed the superior performance of ternary DESs. In particular, the ternary systems ChCl/Urea/EG (1:1:1) and ChCl/Gly/EG (1:1:1), show very high viscosity index (VI > 175), and excellent fluidity at low temperatures (pour points as low as −47°C). These are superior-performing compared to regular mineral base oils. Tribological tests demonstrated that several DESs, notably ChCl/Gly and ChCl/Urea/Gly, significantly reduced the coefficient of friction (μ≈0.170–0.186) through the formation of stable boundary films. Electrochemical analysis using Tafel plots unveiled a critical dichotomy in corrosion behavior towards iron. OA-based DESs caused active dissolution due to their acidic nature, while urea, glycerol, and EG-based DESs induced passivation. Glycerol and EG notably acted as corrosion inhibitors in the aggressive ChCl/OA system, although the ChCl/Urea/EG system exhibited pitting corrosion. This behavior was linked to mass transfer limitations imposed by DES viscosity, influencing both cathodic reactant supply and anodic passive layer formation. Overall, this study highlights that while ternary DESs offer a promising combination of physicochemical and tribological properties for lubrication, their interaction with metal surfaces is a critical design parameter. The choice of HBDs directly dictates the corrosion mechanism, underscoring the necessity for a holistic approach in designing next-generation DES-based lubricants.

1. Introduction

Lubricants are essential materials designed to minimize friction and wear between moving mechanical parts, ensuring the proper performance durability of equipment and finally minimizing the overall energy losses. These materials are highly versatile and can exist in various forms such as liquid, solid, or semi-solid, depending on the specific application. Among these, conventional liquid lubricants (a mixture of mineral base oil, synthetic base oil, and bioderived base oils with additive package) are often preferred for their ease of application, long service life, noise reduction, and heat transfer capabilities (Soni et al., 2014, Shah et al., 2021).

To enhance their performance, the mineral base oils are almost always combined with 5–30% additives of the final product that improve physical, chemical and mechanical properties such as friction coefficient, viscosity index (VI) and provide resistance to oxidation and corrosion (Donato et al., 2021). Petroleum-derived lubricants are hazardous, non-biodegradable, and substantially contribute to greenhouse gas emissions throughout their entire lifecycle, from production to disposal (Nguyen et al., 2024). However, increasing technological demands and growing environmental concerns are encouragement the search for more efficient and sustainable alternatives. In response to these challenges, two innovative classes of materials have developed as highly promising candidates for advanced lubrication applications, named ionic liquids (ILs) and deep eutectic solvents (DESs). These substances possess unique properties that make them suitable for modern lubrication needs (Donato et al., 2021, Cai et al., 2020, Shah et al., 2021).

DESs are a class of green solvents formed by combining hydrogen bond donors (HBDs) with hydrogen bond acceptors (HBAs) (Abbott et al., 2017, Qader, 2021). The resulting mixture has a melting point significantly lower than that of its individual components, forming a liquid at room temperature. DESs share several valuable properties with ILs, such as low volatility and high thermal and chemical stability (Sernaglia et al., 2024). However, DESs are fundamentally distinct from ILs in both chemical composition and intermolecular interactions. ILs are single-component systems consisting solely of discrete cations and anions, with their liquid state stabilized by electrostatic (Coulombic) forces. Conversely, deep eutectic solvents (DESs) are multi-component mixtures often created by amalgamating a hydrogen bond acceptor (HBA), such as choline chloride (a quaternary ammonium salt), with a HBDs, such as urea, ethylene glycol, carboxylic acids, or glycerol. The interaction mechanism of DESs differs fundamentally from the purely ionic nature of ILs. Consequently, the presence of a neutral molecular component and the reliance on hydrogen bonding for eutectic formation categorically exclude DESs from classification as true ionic liquids (Smith et al., 2014, Sernaglia et al., 2024).

Environmentally, DESs share many of the desirable properties of ILs, such as negligible vapor pressure and non-flammability, but are generally regarded as safer due to their low toxicity and the benign nature of their components (Smith et al., 2014). While some mild toxic effects have been noted, DESs were intentionally developed to avoid the toxicity issues often linked to ILs. Moreover, DESs based on ChCl with each of the HBDs, such as urea and glycerol, have demonstrated low corrosiveness, further addressing IL-related limitations. (Ahmed et al., 2017, Sernaglia et al., 2025).

Their ease of recycling also supports their environmentally friendly profile. A major strength of DESs lies in their tunability. By choosing different HBDs and HBAs, researchers can tailor DESs to meet specific lubrication needs. Rather than being static substances, DESs represent a flexible platform that enables the design of task-specific lubricants (Smith et al., 2014). This marks a shift from simply selecting an appropriate lubricant to purposefully engineering an optimal one opening new avenues in lubricant development and innovation. Mineral oil-based lubricants pose significant ecological concerns due to their low biodegradability and high ecotoxicity (Schneider, 2006). In contrast, DESs are generally recognized as biodegradable, owing to the natural origin of many precursor components.

Although comprehensive biodegradability studies on DESs are still in progress, preliminary findings indicate promising results, with certain formulations achieving over 60% biodegradation within 14 days, additionally, the non-toxic nature of DES precursors supports their classification as environmentally benign and safe for human health (Sernaglia et al., 2025). This is especially true for natural deep eutectic solvents, which are derived from renewable sources and represent a more sustainable lubrication solution. Beyond their ecological benefits, DESs exhibit strong performance characteristics, including, cost-effectiveness and ease of synthesis, hydrophobicity and a wide liquid range, enhanced lubricity, a high VI, and reduced evaporative losses, these properties position DESs as a highly promising material class, capable of matching or exceeding the performance of bio-based lubricants while potentially addressing their stability limitations (Sernaglia et al., 2025). DESs which have polar groups such as carboxylic acids, alcohols, amines, esters, and amides, through to interact with metal surfaces either via physical adsorption or chemical interaction, while the hydrocarbon tails extend into the lubricant medium, promoting stable surface coverage and effective lubrication as the case of surfactants in liquid lubricants (Tang et al., 2014).

To date, the lubrication studies in which DESs have been applied as base oil or oil additives has covered only binary DESs systems in which only one kind of HBD mixed with one HBA, however, exploring the ternary systems in which one HBA combined with two different HBDs has not been addressed (Sernaglia et al., 2024, Sernaglia et al., 2025).This study introduces ternary DES systems as high-performance base lubricants, evaluating their performance against mineral base oils and binary DESs. The research establishes a new class of sustainable lubricants, offering a highly effective and environmentally friendly alternative to traditional systems, demonstrating superior tribological properties.

2. Materials and methods

Chemicals in this study were used directly without any further purification. ChCl, EG, urea, and OA were supplied by Biochem (99% France), and Gly was supplied by Scharlab (99.5% Spain). Binary DESs have been prepared between ChCl with different HBDs (ChCl/urea in a 1:2 molar ratio to prepare Reline, ChCl/ EG in a 1:2 molar ratio to prepare Ethaline, ChCl/Gly in a 1:2 mole ratio to prepare Glyceline, and ChCl/ OA in a 1:1 molar ratio to prepare Oxaline. Ternary DESs were prepared as follows, ChCl/urea/Gly in a 1:1:1 molar ratio, ChCl/urea/EG in a 1:1:1 molar ratio, ChCl/Gly/EG in a 1:1:1 molar ratio, ChCl/OA/Gly in a 1:0.5:1 molar ratio, and ChCl/OA/EG in a 1:0.5:1 molar ratio. All mixtures were leaved in oven at 60 °C and periodically shaken until homogeneous solutions were obtained.

Mineral base oils have been supplied by Al-Dora Refinery-Baghdad, Iraq, which has been used as a standard mineral base oil for comparison's sake.

All DES and base oil samples were subjected to comprehensive physicochemical characterization using standardized analytical instruments.

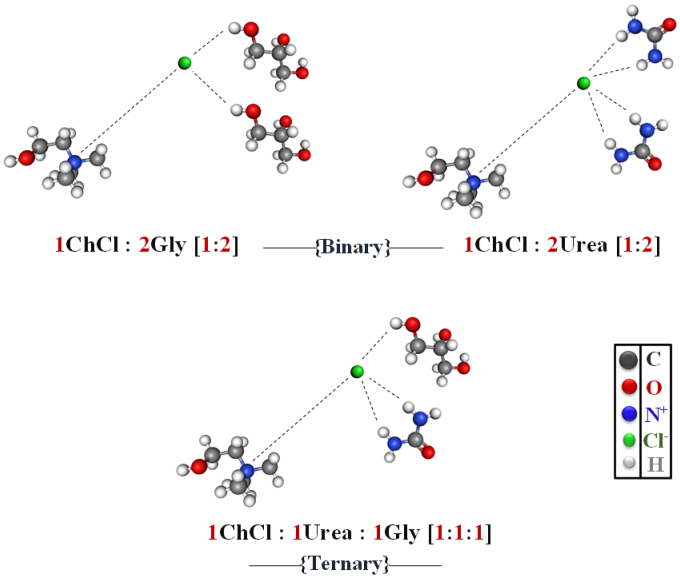

Figure 1: The proposed chemical structure of ternary and binary DESs.

The flash point was determined with a Cleveland Open Cup (COC) Tester (model NCL 440). Density measurements were performed using a Rudolph Density Meter (model DDM 2911). The pour point was assessed employing a CPP CLASSIC apparatus (Norma Lab). Kinematic viscosity was measured using a Houillon Viscometer (Model S-flow IV+).

Subsequently, the viscosity index (VI) of each sample was calculated in accordance with the ASTM D2270 standard test method.;
For liquids with VI = 100 and lower procedure A has been used;

$$VI = ((L - U))/(L - H)) * 100 \quad (1)$$

However, for liquids with VI higher than 100 this equation has been applied.

$$VI = \left[\frac{((antilog\ N\ ) - 1)}{0.00715}\right] + 100 \quad (2)$$

$$N = \frac{(\log H - logU)}{\log Y} \quad (3)$$

L is the kinematic viscosity at 40 °C of an oil of 0 viscosity index having the same kinematic viscosity at 100 °C as the oil whose viscosity index is to be calculated, mm^2/s, **H** is the kinematic viscosity at 40°C of an oil (VI = 100) having the same viscosity at 100°C as the unknown oil, **U** is the kinematic viscosity (mm^2/s) of the oil whose VI is to be calculated at 40°C, and **Y** is kinematic viscosity at 100 °C of the oil whose viscosity index is to be calculated, mm^2 /s.

The inoLab® pH 7110 laboratory pH meter was used to measure the pH of DESs at 25 °C. It measures the electrical potential difference between a reference electrode and a pH electrode. IR spectrums have been recorded by IRTracer-100 Fourier transform infrared (FT-IR). A pin-on-disk tribometer has been used in which, the trials were performed with a standard load of 10 N, a sliding velocity of 0.3 m/s, a sliding radius of 15 mm, and a rotating speed of 191 rpm at ambient temperature. Both the pin and disk were constructed from steel to replicate metal-on-metal contact situations. For corrosion studies, a Corretest CS310M potentiostat/galvanostat has been used. Tafel plots for disc-shape working electrode (made from iron wire 1mm dimeter > 99% from Alfa Aesar) were obtained by sweeping the potential ±300 mV vs. Ag/AgCl (sat.) from corrosion potential (Ecorr.) at a scan rate of 5 mV/s.

3. Results and discussions

Several studies have confirmed the efficiency and endurance of binary DESs used as lubricants and hence laid a foundation for the development of ternary systems. (Lawes et al., 2010) first presented that ChCl–based DESs were capable of reaching low friction coefficients similar to commercial oils for steel/steel contacts. (Ahmed et al., 2017, Abbott et al., 2014) confirmed the low corrosion rates and tribological effectiveness of ChCl–based DESs, and (Li et al., 2022, Li et al., 2023) confirmed that modifications of HBDs like urea and thiourea significantly affected friction reduction and wear protection. (Zhang et al., 2023) Imidazole-based DESs show promise as green, stable, and effective solid lubricants, potentially replacing conventional cutting fluids while being safer and more environmentally friendly, these studies underscore the sound foundation laid by binary DESs for the development of ternary DESs applications within tribological research. Subsequently, (Sernaglia et al., 2024) underscored the need to prepare non-corrosive solutions, represented by choline acetate-based DESs, revealing greater tribological performance.

FT-IR analysis

To validate hydrogen bonding interactions in both binary and ternary DESs, the FT-IR spectroscopy technique has been used to examine the absorption bands associated with HBDs and acceptors, thereby providing supportive indications of the development of complexes within DESs systems (Wang et al., 2019).

The FT-IR spectra of ChCl/Urea, ChCl/Gly and ChCl/Urea/Gly DESs with the characteristic band, along with their vibration assignments, are shown in Figures, and the results are summarized for all DESs in Table 1.

The FT-IR spectra of the ChCl/urea system in Figure 2, offers essential insights into the molecular interactions between the two constituents.

In the spectra of pure urea, three prominent absorption bands are seen at 3427 cm^{-1} and 3328 cm^{-1}, corresponding to the N–H stretching vibrations of the amide group.

The band at 3251 cm^{-1} is ascribed to the asymmetric bending vibrations of the $–NH_2$ groups. Upon development of the ChCl/urea deep eutectic solvent, significant changes in the position and width of these bands occur, suggesting the presence hydrogen bonding interactions between ChCl and urea molecules.

These interactions lead to a more complex vibrational landscape, indicating that the molecular environment has shifted. Additionally, the alterations in absorption characteristics suggest that the solvation dynamics within the deep eutectic solvent are significantly influenced by the formation of new intermolecular interactions. The peaks are notably expanded and displaced to lower wavenumbers: 3420 cm^{-1}, 3315 cm^{-1}, and 3188 cm^{-1}. The red shift indicates a reduction in the strength of the N–H bond resulting from the establishment of large hydrogen-bonding networks between the chloride anion of ChCl and the $–NH_2$ groups of urea.

Additionally, the distinctive peaks of urea at 1680 cm^{-1} and 1591 cm^{-1}, representing the symmetric and asymmetric bending vibrations of the NH_2 groups, respectively, exhibit significant changes to 1660 cm^{-1} and 1603 cm^{-1} in the DES. This suggests the presence of hydrogen bonding and possible rearrangements in the ChCl/urea system. Such changes are consistent with the formation of a hydrogen-bonded network, which is characteristic of deep eutectic solvents(Zhang et al., 2016, Li et al., 2023, Qader et al., 2024) confirming the reason behind the low melting point of eutectic solvent systems.

In Figure 3, the pure hydrogen bond acceptor (ChCl) has several functional groups absorption band, including a vibrational band at 3219 cm^{-1} for –OH stretching and bands at 3025 and 3006 cm^{-1} for N–H stretching. The band in ChCl at 950 is attributed to the asymmetric and symmetric stretching modes of $C–N^+$.

The FT-IR spectra of ChCl/Gly system is primarily characterised by a change in glycerol spectra, which shows a wide band at 3289 cm^{-1} ascribing to O–H groups. This groups are responsible for the formation of a significant network interactions via hydrogen bonds and dipole-dipole interactions among glycerol molecules, giving it high viscosity (Ferreira et al., 2017, Rahmalia et al., 2022).

When 2 moles of glycerol are combined with 1 mole of ChCl, the initial hydrogen bonds between glycerol molecules (OH(Gly)–O(Gly)) are weakened due to the formation of new hydrogen bonds between glycerol hydroxyl groups and chloride ions (OH(Gly)–Cl)(Vieira et al., 2015). This decrease is reflected in the spectra by a slight reduction in both transmittance % and width, accompanied by a minor shift to 3304 cm^{-1}, Characteristic peaks of C–H bonds are observed at 2934 and 2878 cm^{-1}, and they remain unchanged, indicating a minimal effect on aliphatic C-H bonds. In conclusion, the results indicate that ChCl/Gly -DES was formed (Rahmalia et al., 2022, Wang et al., 2019).

The FT-IR spectra of the ChCl/urea/glycerol system in Figure 4 offers substantial information about the molecular interactions among the three components. In the range above 3000 nm, the spectra of pure urea displays three prominent absorption bands at 3427 cm^{-1} and 3328 cm^{-1}, which correspond to the N–H stretching vibrations of the amide group(Li et al., 2023). The band at 3251 cm^{-1} is attributed to the asymmetric bending vibrations of the $–NH_2$ groups .in other hand have glycerol spectra, which shows a wide band at 3289 cm^{-1} ascribing to O–H groups (Rahmalia et al., 2022). Upon formation of the Ternary DES, these vibrations show noticeable shifts to 3324 and 3203 cm^{-1}, where the N–H and O–H stretching bands overlap. This shift to lower wavenumbers, along with pronounced peak broadening, is indicative of enhanced hydrogen-bonding interactions within the solvent system. Such changes reflect a structural reorganization in the DES, confirming the effective interaction between urea, glycerol, and other components, which contributes to the unique physicochemical properties of the resulting solvent. Additionally, the distinctive peaks of urea at 1680 cm^{-1} and 1591 cm^{-1}, representing the symmetric and asymmetric bending vibrations of the NH_2 groups, respectively, exhibit significant changes to 1660 cm^{-1} and 1603 cm^{-1} in the DES.

The FT-IR analysis further suggests that the establishment of DES does not lead to the formation of new functional groups in the mixture.

Three main observations indicate that ChCl, urea, and glycerol remain chemically unchanged and only interact through hydrogen bonding. ChCl's ammonium peak at 950 cm^{-1} confirms strong hydrogen bond formation. Urease's carbonyl stretching vibrations show hydrogen bond interactions without structural

alteration. Glycerol's C–H stretching peaks at 2943 and 2875 cm^{-1} further support hydrogen bonding among the components.

Table 1 : Characteristic band assignment of the FT-IR for deep eutectic solvents (DESs)

Urea	ChCl-urea BDES	Assignment	Glycerol	ChCl-Gly BDES	Assignment
3427cm^{-1}	3420cm^{-1}	-NH_2 stretching	3289cm^{-1}	3304cm^{-1}	O-H stretching
3328cm^{-1}	3315cm^{-1}	-NH_2 stretching	2934cm^{-1}	2934cm^{-1}	C-H stretching
3251cm^{-1}	3188cm^{-1}	-NH_2 bending vibration	2878cm^{-1}	2878cm^{-1}	C-H stretching
1680cm^{-1}	1660cm^{-1}	-NH_2 bending symmetric			
1591cm^{-1}	1603cm^{-1}	-NH_2 bending asymmetric			
Ethylene Glycol (EG)	ChCl-EG BDES	Assignment	Oxalic acid	ChCl-OA BDES	Assignment
3297cm^{-1}	3300cm^{-1}	O-H stretching	3417cm^{-1}	3335cm^{-1}	O-H stretching
2938cm^{-1}	2938 cm^{-1}	C-H stretching	1610 cm^{-1}	1723cm^{-1}	C=O stretching
2874cm^{-1}	2870cm^{-1}				
Urea	Ethylene Glycol (EG)	ChCl:Urea:EG TDESs	Glycerol	Ethylene Glycol (EG)	ChCl:Gly:EG TDESs
3427cm^{-1}	3297cm^{-1}	3324cm^{-1}	3289cm^{-1}	3297cm^{-1}	3302cm^{-1}
3328cm^{-1}		3206cm^{-1}	2934cm^{-1}	2938cm^{-1}	2934cm^{-1}
			2878cm^{-1}	2874cm^{-1}	2875cm^{-1}
3427cm^{-1}	2938cm^{-1}	2938cm^{-1}			
	2874cm^{-1}	2875cm^{-1}			
1680cm^{-1}		1662cm^{-1}			
1591cm^{-1}		1614cm^{-1}			
Glycerol	Oxalic acid	ChCl:Gly:OA TDESs	Oxalic acid	Ethylene Glycol (EG)	ChCl:OA:EG TDESs
3289cm^{-1}	3417cm^{-1}	3312cm^{-1}	3417cm^{-1}	3297cm^{-1}	3312cm^{-1}
2934cm^{-1}		2938cm^{-1}		2938cm^{-1}	2948cm^{-1}
2878cm^{-1}		2882cm^{-1}		2874cm^{-1}	2874cm^{-1}
	1610 cm^{-1}	1740 cm^{-1}	1610 cm^{-1}		1741 cm^{-1}

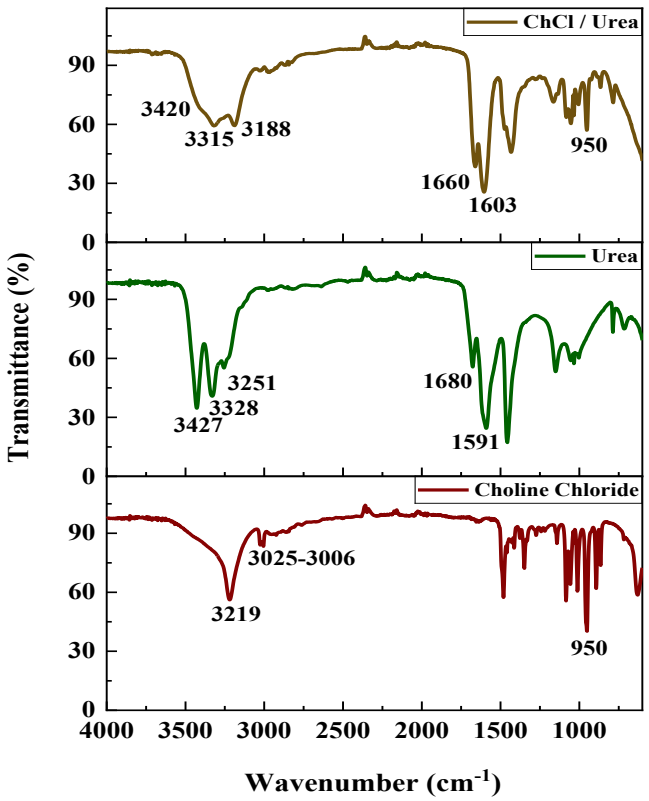

Figure 2 : FT-IR spectra of ChCl /Urea

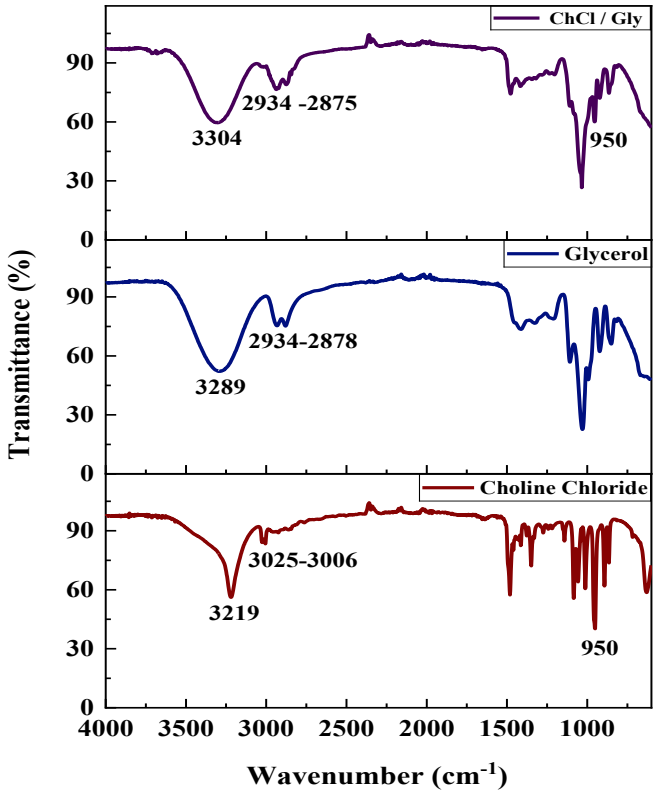

Figure 3 : FT-IR spectra of ChCl /Glycerol

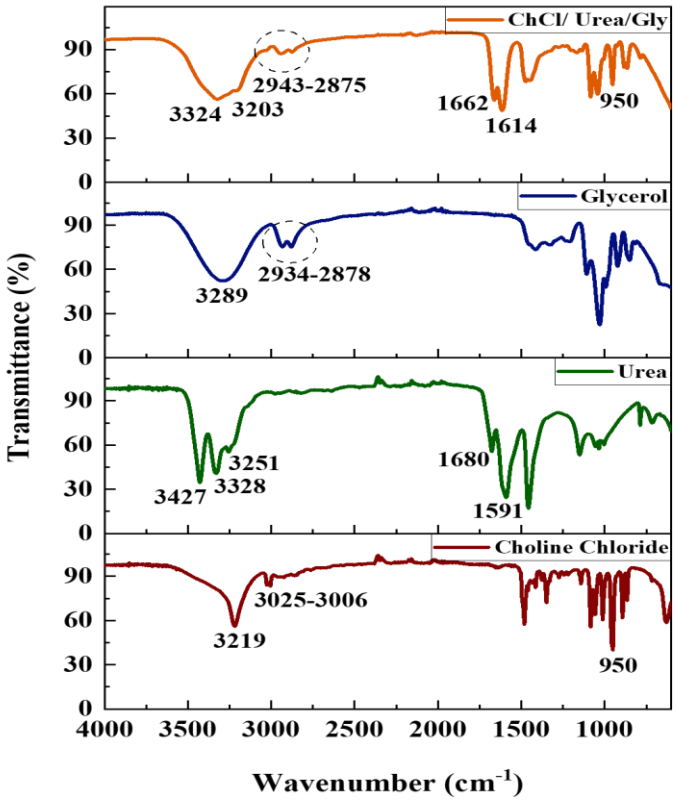

Figure 4 : FT-IR spectra of ChCl/Urea /Glycerol

Physicochemical properties of liquids

Viscosity

Viscosity is an important property of liquid for the formation of lubricating film and minimizing wear in lubricated systems. The effect of viscosity in lubricating oils is often characterized by its variation with temperature, known as the viscosity index (VI). A high VI signifies minimal viscosity changes as temperature rises representing that the lubricant preserves its viscosity more effectively over a wide range of operational temperatures (Liu et al., 2024). Compared to most solvents, DESs are highly viscous due to their strong hydrogen bonding, dipole-dipole and London force interactions (Zhang et al., 2012, Wang et al., 2019). Based on these interactions, DESs show a broad range of viscosity and much better VI than conventional base oils.

Table 2 shows that binary DESs like ChCl/urea have very high viscosities but not too much VI, while ChCl/EG has low viscosity but has high VI (216.92). Ternary DESs such as ChCl/urea/EG and ChCl/Gly/EG possess a balanced profile and possess moderate

viscosities along with maximum VI (175–185), representing balanced lubrication conditions. On the other hand, mineral base oils such as SN150, SN500, and bright stock possess low VI levels (92–99), which mean they significantly lose their viscosity with a rise in temperature compared with DESs used. TDESs have much higher VI than mineral base oils, however lower than binary DESs. This could be attributed to the re-establishment of intermolecular forces when two type of HBDs are involved in the formation of TDES system, All TDESs exhibit very high VI (158-186), this indicates excellent viscosity stability, which is the main characteristic of these DES formulations.

Table 2 : Physicochemical and lubrication properties of liquids.

Liquid groups	liquids	Density (g/ml) at 25 °C	Viscosity mm^2s^{-1}		Viscosity index	Pour point °C	Flash point °C	PH at R. T	average friction coef. (μ)
			at 40 °C	at 100 °C					
A	ChCl/urea	1.19820	215	23	131.40	-3	114	8.53	0.211
	ChCl/Gly	1.19457	112	20	202.89	-34	144	6.81	0.170
	ChCl/EG	1.12146	18.1	4.9	216.92	-45	133	5.12	0.279
	ChCl/OA	1.23145	142	21.8	180.84	4	105	- 0.35	0.281
B	ChCl/urea/Gly	1.19215	102.7	15.4	158.58	-25	158	7.38	0.186
	ChCl/urea/EG	1.15619	44.96	8.67	175.12	-35	160	6.22	0.282
	ChCl/Gly/EG	1.15546	40.98	8.34	185.14	-47	160	4.23	0.243
	ChCl/OA/Gly	1.20869	55.08	10.36	180.11	-32	116	0.70	0.211
	ChCl/OA/EG	1.17282	25.12	5.8	186.34	-46	116	0.20	0.236
C	SN150/Stock 40	0.8586	15.7	3.5	99.09	-4	194	-	0.242
	SN500/Stock 60	0.88261	63.2	8.20	96.93	-4	224	-	0.217
	Br Stock	0.90724	370.8	25.8	92.30	0	274	-	0.275

Density

Measuring the density of base oils is critical for several reasons. It directly influences blending care, as accurate density measurements are important for correct additive dosing, ensuring the desired viscosity and optimal lubricant performance.

Density also plays an important role in storage and transport efficacy by determining the weight/volume ratio, which influences container sizing, logistics, and related costs. In addition, measuring density is an important factor in maintaining quality, as unanticipated density changes can specify contamination, oxidation, or in the refining irregularities. Finally, density is vital for preparation compatibility, affecting base oils/additives interact, thus affecting miscibility and stability during blending (Morais et al., 2020).

Low-density oils offer better flow and energy efficiency but may be less protective under extreme conditions such as high pressure, elevated temperatures, or severe mechanical stress. High-density oils on the other hand, improve film strength and load capacity but may be heavier, less efficient, or harder to pump.

Table 2 shows that the traditional base oils possess a density from 0.85-0.90 g/mL and are primarily comprised of non-polar hydrocarbons. These low-density lubricants exhibit poor surface interaction and less physical adsorption onto metal surfaces, which can impair their performance in extreme environments or corrosive atmospheres. DESs which are derived from ChCl with HBDs such as urea, glycerol, or ethylene glycol, have much greater densities, usually more than 1.15 g/mL. DESs are able to

form boundary films on metal surfaces, thereby reducing metals' direct contact and enhancing anti-wear characteristics. Denser fluids also have greater momentum transfer and vaporisation resistance at high temperature and pressure, which enhance thermal stability and sealing efficiency.

All DESs have higher densities than mineral base oils (Sernaglia et al., 2025). In addition, factors such as temperature (Shahbaz et al., 2011), water content, and the preparation method (Florindo et al., 2019) significantly influence these properties .

Pour point

The pour point of lubricating base oils is an essential characteristic, mainly in cold environments, as it defines the lowest temperature at which the oil remains fluid enough to flow under normal conditions. When temperatures drop below the pour point, the oil can thicken or even solidify, weakening its ability to lubricate effectively. This can result in difficulty in starting engines, increased mechanical wear, higher energy usage and potentially severe equipment failure. Selecting the appropriate lubricant, particularly one with a pour point lower than the lowest expected operating temperature, is critical for consistent performance in cold climates, as well as during transportation and storage. Furthermore, it acts as an important quality benchmark. For adequate performance, additives or synthetic oil formulations are often employed to improve cold-temperature performance, enhancing equipment reliability and extending service life (Sad et al., 2014). A reduced pour point is beneficial for lubricants and hydraulic fluids, as it ensures enhanced fluidity and performance at low temperatures (Sokolnikov et al., 2016).

Table 2 shows that group A liquids have excellent potential for low-temperature applications. ChCl/EG has an exceptionally low pour point of -45°C. However, ChCl/OA is inappropriate for cold conditions with a pour point of 4°C. TDESs exceeds in low-temperature performance, with pour points ranging from -25°C to -47°C. This makes them superior to some binary DESs and of course, conventional oils for cold-start applications. The pour points of mineral base oils (-4°C to 0°C) are significantly not as good as most of the DESs, indicating lesser performance in cold conditions.

Flash point

Measuring the flash point of lubricating base oils is important for assessing thermal suitability for their applications, detecting contamination or formulation issues, ensuring safe handling and storage, and maintaining regulatory compliance and quality control (Liu and Liu, 2010).

Table 2 shows that both binary and ternary DESs have lower flash points than mineral base oils. This is because, unlike DESs, mineral base oils are composed mainly of long-chain hydrocarbon molecules, which makes them less volatile. However, the components of DESs are smaller in size than mineral base oil, but they get their high viscosity due to their strong intermolecular network. It could be noted that, all binary and ternary DESs containing OA have low flash points because OA breaks down into formic acid, carbon monoxide, carbon dioxide, or formaldehyde when heated above 100°C (Schuler et al., 2023).

However, when ternary DESs are combined with additional HBDs, the buoyancy point is often enhanced. The ternary DESs provide more stable hydrogen-bonding networks due to the synergistic interactions among the three components. In such systems, the presence of multiple HBDs and a HBA allows for the formation of diverse bonding arrangements, which enhance structural stability, which reduces structural volatility and increases the buoyancy point. While they do not attain the flash point of base oils, they markedly improve the efficacy of binary DESs and provide an enhanced safety profile. Using more stable HBDs or additives to enhance hot areas may be an effective strategy for safer DES-based lubricants.

Friction tests

Reducing friction and wear is essential for efficiency, reducing energy use, and the longevity of machinery (Gohar and Rahnejat, 2018). The assessment of tribological performance is generally conducted using wear testers, which replicate contact conditions between lubricated surfaces under regulated pressure, velocity, and

temperature, thereby producing data on wear scar diameter and friction coefficient. This establishes a scientific framework for evaluating and enhancing lubricant performance. Lubricants form a stable, resistant film on machine surfaces, protecting them from direct metal-to-metal contact.

The friction coefficient measurement results are shown in Figures 5 and 6. It could be noted that when there is no lubricant, the friction values are often the highest and most unpredictable, starting over μ = 1.2, which means there is a lot of surface contact and poor performance in terms of wear and tear. Conversely, both binary (Figure 5) and ternary (Figure 6) DESs formulations, demonstrate noticeably lower and more consistent friction coefficients over the entire testing period. Among DES systems, ChCl/Urea, ChCl/Gly, ChCl/Urea/Gly, and ChCl/OA/Gly exhibited the most persistent decrease in friction, coefficients (μ ranges from 0.170 and 0.186) outperforming all base oils. The stability of these DESs over long sliding distances shows that they are efficient at forming a protective layer and providing lubrication, making them appealing choices for eco-friendly and effective lubrication solutions. As mentioned before, "This behaviour may be ascribed to their plethora of strongly adsorptive functional groups, which promote substantial interactions with the lubricated surfaces." (Tang et al., 2014).

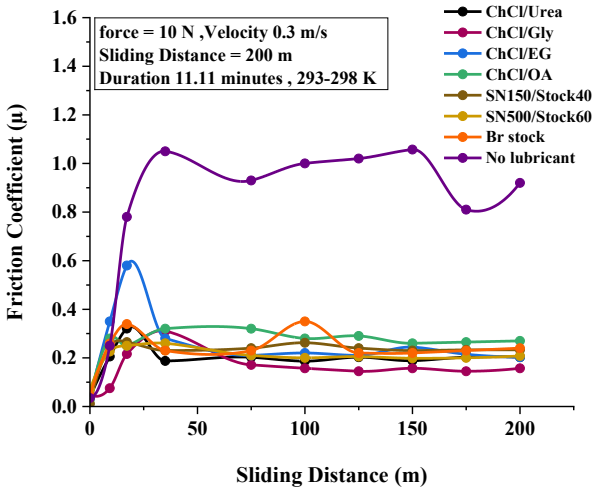

Figure 5: Friction coefficient of binary DESs with base oils.

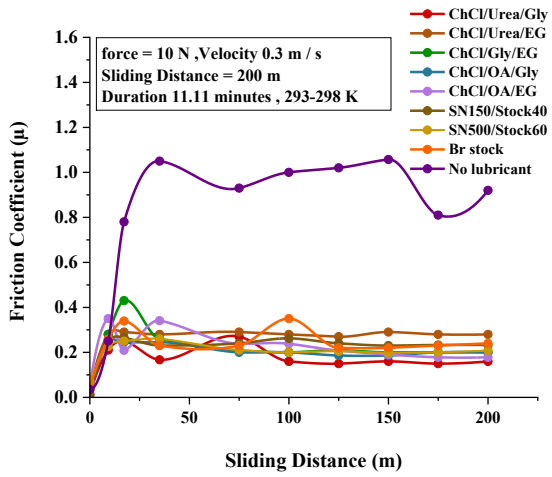

Figure 6 : Friction coefficient of Ternary DESs with base oils.

Figure 7 illustrates the average friction coefficients (μ) for several lubricants under consistent testing conditions. The lack of lubrication yields the highest average friction coefficient of 0.868, serving as the reference point for comparison.

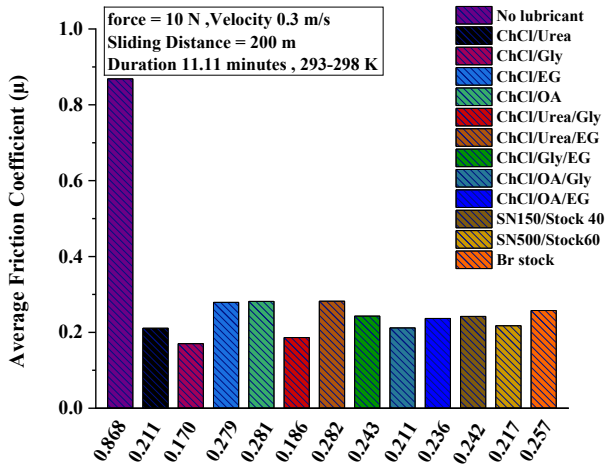

Figure 7: Average friction coefficient of binary and ternary DESs compared with mineral base oils.

Among mineral base oils tested, SN500 shows the lowest friction coefficient, which is 0.217, indicating a significant improvement friction reduction (65.1%). On the other hand, most of the DESs studied in this study had better properties for reducing friction, as shown by their

lower friction coefficients compared to the reference lubricant. For example, ChCl/Gly achieves a markedly reduced value of μ = 0.170, indicating a 70% reduction compared to unlubricated surface and ChCl/Urea/Gly has μ ≈ 0.186, which is almost 68.2% lower than lubricant-free surface. These findings indicate that some DESs outperform base oils in terms of friction.

The benefit arises from their capacity to establish stable boundary layers, enhance hydrogen bonding interactions, and demonstrate superior surface compatibility, making them ideal candidates for modern and eco-friendly lubricating systems.

Corrosion studies

Although many metals are involved, iron (as cast iron and steel) remains the foundational metal in most engine components (Gupta et al., 2017). Here, we are addressing how is iron susceptible to corrosion in environments in which binary or ternary DESs are used as base lubricants at room temperature using linear sweep voltammetry (LSV). Figure 8, shows the electrochemical corrosion behavior of iron in various binary DESs at room temperature as Tafel plots.

Significant differences in corrosion resistance were observed depending on the nature of the HBD in the DES. Based on the height of corrosion currents, the ChCl/OA DES system exhibited the highest corrosion rate among all tested environments. As shown in Tafel plots, the ChCl/OA curve (light grey line) is significantly shifted to the right (more positive potentials), and have the most higher corrosion current density (i_{corr}) among other DES systems. This high i_{corr} signifies a drastically faster rate of iron corrosion in this solvent system.

The anodic part of the ChCl/OA system (potentials above corrosion potential (E_{corr})) displayed a steep and continuous increase in current density, representative of active dissolution. This behavior suggests that iron corrodes rapidly without forming a protective film. The pronounced corrosivity of ChCl/OA known as Oxaline can be ascribed to the acidic nature of OA, a HBD, which leads to an elevated proton (H^+) concentration (Saltykov et al., 2004, Ashrafi et al., 2008).

These protons are readily reduced in the cathodic reaction ($2H^+ + 2e^- \rightarrow H_2$), consuming electrons loosed by iron, thereby accelerating the corresponding anodic Fe corrosion reaction to maintain charge balance. Furthermore, the formation of detachable insoluble iron oxalate complexes by Fe^{2+} ions likely prevents the establishment of a protective passive layer on the iron surface (Ahmed et al., 2021).

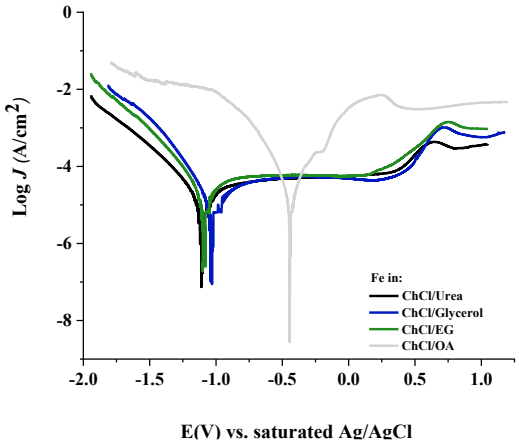

Figure 8 : Tafel plots of iron in Binary DESs

On the other hand, in contrast to the ChCl/OA system, the ChCl/Urea, ChCl/Glycerol, and ChCl/ EG DESs showed remarkably improved corrosion resistance. The Tafel for these three DES systems (black, blue, and green lines, respectively) are located at significantly lower current densities (shifted further to the left) compared to the ChCl/OA curve, indicating substantially lower corrosion rates (lower i_{corr}).

An important feature observed in these three systems is the passivation behavior in their anodic branches. Following an initial increase in current, the current density either leveled off or decreased, forming a characteristic plateau. This phenomenon signifies the formation of a thin, stable, and protective or semi-protective film on the iron surface, likely an oxide or hydroxide layer. This film acts as a barrier, effectively slowing down further corrosion even with increasing potential (Abbott et al., 2014, Ahmed et al., 2021).

For comparison's sake, while all three DESs (ChCl/Urea, ChCl/Glycerol, and ChCl/EG)

are significantly less corrosive than ChCl/OA, understated differences exist among them. The E_{corr} for all three passivating solvents was found to be similar and notably more negative (less noble) than the E_{corr} observed in ChCl/OA. Concerning the i_{corr}, ChCl/Glycerol and ChCl/EG showed the lowest values, suggesting superior corrosion protection within this group. The i_{corr} for ChCl/Urea was slightly higher than that of the Glycerol and EG systems, indicating a marginally increased corrosion rate. Furthermore, the passive regions for the Glycerol and EG systems appeared to be slightly more defined than for the Urea system, suggesting a more robust and stable passive film formation.

Based on the Tafel plots, the corrosivity of these DESs towards Fe at room temperature can be ranked as follows (most corrosive: ChCl/OA >> ChCl/Urea > ChCl/Glycerol ≈ ChCl/EG).

Conversely, ChCl/Glycerol and ChCl/EG offer the best corrosion protection, closely followed by ChCl/Urea. The chemical characteristics of the HBD in the DES strongly influence the extent and mechanism of iron corrosion (Abbott et al., 2014, Ahmed et al., 2021). The acidic nature of OA made a highly aggressive and corrosive environment leading to active dissolution. In contrast, urea, glycerol, and EG enable the formation of a passive film on the iron surface, providing significant protection against corrosion, with Glycerol and EG-based DESs demonstrating slightly superior performance (Ahmed et al., 2021).

Kinetically, the corrosion behavior of metals in DESs is influenced by a number of factors including, physicochemical properties of medium, ambient conditions, and the features of the metal substrate. The principal coordinating ligand, such as the chloride ion, is essential in influencing the metal's electrochemical behavior. Anodic dissolution kinetics are governed by the type and ligand and its activity in the medium, whereas DES properties such as density, viscosity, and acidity control mass transport (Abbott et al., 2015). These parameters finally, influence the configuration of Tafel plots (Bučko and Bajat, 2022).

Figure 9 presents the Tafel plots for iron immersed in various ternary DESs. The results clearly differentiate between passivating and corrosive systems based on their i_{corr} values. The passivating systems for iron shown as black line for (ChCl/Urea/Gly), blue line for (ChCl/Urea/EG), and green line for (ChCl/Gly/EG) curves, exhibit significantly lower i_{corr} values, indicating reduced corrosion rates. Their curves are shifted to the left, signifying slower kinetics. For instance, ChCl/Urea/Gly (black line) and ChCl/Gly/EG (green line) demonstrate classic passivation behavior, where the anodic current initially increases (active dissolution) before decreasing or plateauing to form a stable passive region. This suggests the formation of a robust, protective film on the iron surface that effectively mitigates corrosion over a broad range of potentials.

Conversely, the corrosive systems, represented by the white (ChCl/OA/Gly) and magenta (ChCl/OA/EG) curves, show substantially higher i_{corr} values, reflecting elevated corrosion rates, and are shifted far to the right. These curves display no evidence of passivation, with current density continuously increasing with potential in the anodic branch, characteristic of active dissolution.

A noteworthy trend is observed in the electrochemical behavior of iron within the ChCl/Urea/EG system (blue line), while it initially forms a passive region, a sharp and sudden increase in current density occurs around -0.3 V. This indicates pitting corrosion, where the passive film breaks down locally at a specific breakdown potential (E_{pitt}) leading to highly localized and rapid corrosion.

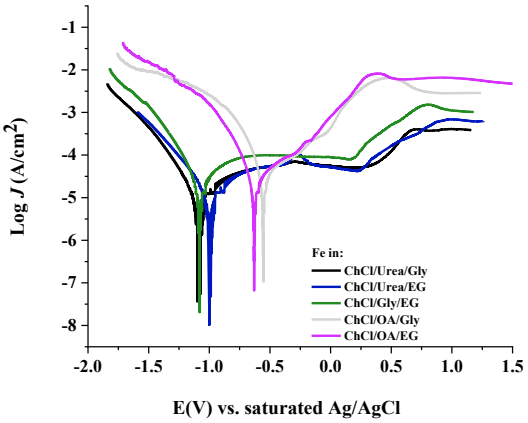

Figure 9: Tafel plots of iron in Ternary DESs

The significantly lower i_{corr} values observed for the ChCl/Urea/Gly, ChCl/Gly/EG, and ChCl/Urea/EG systems, confirm their passivating nature, consistent with their binary counterparts (ChCl/Urea, ChCl/Gly, ChCl/EG). These systems exhibit a less noble (more negative) E_{corr}, indicating a thermodynamic tendency for corrosion. However, the formation of a stable passive film kinetically hinders the corrosion process. The classic passivation behavior, characterized by an initial increase in current followed by a plateau or drop in the anodic branch, signifies the formation of a protective layer on the iron surface. This film remains intact over a wide potential range, effectively slowing down metal dissolution.

In contrast, the high i_{corr} values of the ChCl/OA/Gly and ChCl/OA/EG systems are comparable to the highly corrosive binary ChCl/OA system. These systems show no passivation, with continuous current density increase, indicative of free metal dissolution due to the aggressive, acidic nature of the OA-containing DESs. The more positive E_{corr} values in these systems are attributed to a very fast cathodic reaction, specifically the reduction of (H^+) from the acid, which shifts the overall potential to a more noble value despite the high corrosion rate. Despite their high corrosivity, the addition of glycerol or EG to the ChCl/OA system (white and magenta curves) resulted in a slight leftward shift in their Tafel plots compared to the binary ChCl/OA system.

This indicates a reduction in i_{corr}, demonstrating that Gly and EG act as corrosion inhibitors in this aggressive environment. Similar to polyols, these HBDs can adsorb onto the iron surface, thereby forming an adsorbed layer that acts as a protective barrier against corrosion (Tang et al., 2014). This adsorbed layer blocks active sites, slowing down both the anodic (iron dissolution) and cathodic (proton reduction) reactions, thereby decreasing the overall corrosion rate. While not potent enough to induce passivation in such a highly acidic medium, they successfully mitigate corrosion.

The observed corrosion behaviors are significantly influenced by the physicochemical properties of the DESs, particularly mass transfer limitations due to viscosity. In the highly corrosive ChCl/OA system, the primary cathodic reactant is H^+ ions. Although its concentration is high, the overall reaction rate can be limited by the slow diffusion of protons through the viscous liquid to the iron surface, a phenomenon known as mass-transfer limitation or diffusion control. This effect is clearly shown from the difference between ChCl/OA/EG and ChCl/OA/Glycerol plots, in which the corrosion of Fe in the ChCl/OA/EG system is shown to be higher than the ChCl/OA/Glycerol system. This is clearly correlated to the lower viscosity profile of EG compared with the viscosity of glycerol (Abbott et al., 2014).

For the passivating systems (ChCl/Urea, Gly, and EG-based), the cathodic reactant is likely dissolved oxygen (O_2) or trace amounts of H_2O. The low solubility and slow diffusion of O_2 in these viscous DESs mean that the entire corrosion process is under cathodic mass-transfer control (the plateaued part of the plot is under the control of this phenomenon). Corrosion can only proceed as fast as O_2 is supplied to the surface, explaining the significantly lower i_{corr} values compared to the H^+-rich ChCl/OA system. Furthermore, slow diffusion in viscous DESs is critical for the anodic reactions and the formation of passive films. The Fe^{2+}, ions produced during initial corrosion accumulate at the metal-liquid interface due to their slow dispersion into the bulk solution. This supersaturation, along with the presence of species like OH^- or oxide ions, promotes the precipitation of a solid iron oxide/hydroxide film directly onto the surface, which is the key to passivation. This slow mass transfer of corrosion products away from the surface facilitates the formation of a stable protective layer(Hamadi et al., 2018). In less viscous solvents, these ions would diffuse away too quickly for a stable film to form, explaining the distinct passive regions in the Urea, Glycerol, and EG-based systems.

The pitting corrosion observed in the ChCl/Urea/EG system (blue curve) is also influenced by mass transfer. Pitting typically occurs due to the local breakdown of the passive film, often instigated by the migration and accumulation of aggressive anions, such as Cl^- (abundant from ChCl) (D'Agostino et al., 2015). In

viscous DESs such those containing urea and Gly as HBDs and in their ternary systems, slow diffusion can lead to localized Cl^- accumulation at weak points in the passive film, triggering pit formation. Once a pit forms, the corrosion within it is extremely fast (Frankel, 1998, Trethewey and Chamberlain, 1995). The geometry of pits further restricts mass transfer, trapping corrosive species and preventing inhibitors or passivating agents from reaching the localized area, creating a self-sustaining aggressive environment. The sharp, vertical increase in current density on the blue curve is a characteristic indicator of this rapid, localized corrosion.

Conclusion

This study successfully synthesized and evaluated a range of binary and novel ternary DESs, advancing their potential as sustainable, high-performance lubricants. The ternary DESs, particularly ChCl/Urea/EG and ChCl/Gly/EG, showed superior physicochemical and tribological properties, including high viscosity indices (>175), excellent low-temperature operability (pour points down to -47 °C), and up to 70% reduction in friction coefficient, outperforming traditional mineral oils. Central to the observed corrosion behavior was the identity of the HBD, as its chemical nature governs parameters such as acidity/basicity, complexation ability, and surface affinity. These characteristics strongly influence the stability of the protective layer formed at the metal–electrolyte interface, thereby dictating whether the system promotes passivation, uniform corrosion, or localized pitting. While OA induced severe corrosion through active iron dissolution, HBDs such as urea, Gly, and EG promoted the formation of protective passive films, significantly mitigating corrosion. Interestingly, Gly and EG also demonstrated an ability to inhibit corrosion even in otherwise aggressive systems. Nevertheless, specific combinations, such as ChCl/Urea/EG, exhibited susceptibility to localized pitting, thereby highlighting the intricate interrelationship between HBD chemistry and the stability of the protective film. The high viscosity of DESs played a dual role, retarding corrosion through mass transfer limitations while concurrently aiding passivation. Collectively, these findings underscore the promise of DESs as next-generation lubricants, but they also highlight the necessity of holistic design strategies that consider not only bulk fluid properties but also nuanced electrochemical interactions at the fluid-metal interface. Continued research is needed to engineer DES formulations that integrate excellent lubrication performance with robust corrosion resistance, paving the way for their practical deployment in environmentally conscious lubrication technologies.

Acknowledgment

Authors would like to acknowledge the financial support of the chemistry department, College of Education, Salahaddin University-Erbil, KRG, Iraq and Al-Dora Refinery.

Conflict of interest

The author declares no conflict of interest.

References

ABBOTT, A. P., AHMED, E. I., HARRIS, R. C. & RYDER, K. S. 2014. Evaluating water miscible deep eutectic solvents (DESs) and ionic liquids as potential lubricants. *Green Chemistry,* 16(9)**,** 4156-4161.

ABBOTT, A. P., AHMED, E. I., PRASAD, K., QADER, I. B. & RYDER, K. S. 2017. Liquid pharmaceuticals formulation by eutectic formation. *Fluid Phase Equilibria,* 448(2-8.

ABBOTT, A. P., FRISCH, G., HARTLEY, J., KARIM, W. O. & RYDER, K. S. 2015. Anodic dissolution of metals in ionic liquids. *Progress in natural science: Materials international,* 25(6)**,** 595-602.

AHMED, E. I., ABBOTT, A. P. & RYDER, K. S. Lubrication studies of some type III deep eutectic solvents (DESs). AIP Conference Proceedings, 2017. AIP Publishing LLC, 020006.

AHMED, E. I., RYDER, K. S. & ABBOTT, A. P. 2021. Corrosion of iron, nickel and aluminium in deep eutectic solvents. *Electrochimica Acta,* 397(139284.

ASHRAFI, A., GOLOZAR, M. & MALLAKPOUR, S. 2008. EIS investigation of passive film formation on mild steel in oxalic acid solution. *Journal of Applied Electrochemistry,* 38(225-229.

BUČKO, M. & BAJAT, J. 2022. A review of the electrochemical corrosion of metals in choline chloride based deep eutectic solvents. *Journal of Electrochemical Science and Engineering,* 12(2)**,** 237-252.

CAI, M., YU, Q., LIU, W. & ZHOU, F. 2020. Ionic liquid lubricants: when chemistry meets tribology. *Chemical Society Reviews,* 49(21)**,** 7753-7818.

D'AGOSTINO, C., GLADDEN, L. F., MANTLE, M. D., ABBOTT, A. P., ESSA, I. A., AL-MURSHEDI, A. Y. & HARRIS, R. C. 2015. Molecular and ionic diffusion in aqueous–deep eutectic solvent mixtures: probing inter-molecular interactions using PFG NMR. *Physical Chemistry Chemical Physics,* 17(23)**,** 15297-15304.

DONATO, M. T., COLACO, R., BRANCO, L. C. & SARAMAGO, B. 2021. A review on alternative lubricants:

Ionic liquids as additives and deep eutectic solvents. *Journal of Molecular Liquids,* 333(116004.
FERREIRA, A. G., EGAS, A. P., FONSECA, I. M., COSTA, A. C., ABREU, D. C. & LOBO, L. Q. 2017. The viscosity of glycerol. *The Journal of Chemical Thermodynamics,* 113(162-182.
FLORINDO, C., BRANCO, L. C. & MARRUCHO, I. M. 2019. Quest for green-solvent design: from hydrophilic to hydrophobic (deep) eutectic solvents. *ChemSusChem,* 12(8)**,** 1549-1559.
FRANKEL, G. 1998. Pitting corrosion of metals: a review of the critical factors. *Journal of the Electrochemical society,* 145(6)**,** 2186.
GOHAR, R. & RAHNEJAT, H. 2018. *Fundamentals of tribology*, World Scientific
GUPTA, A., SHARMA, S. & NARAYAN, S. 2017. Combustion Engines: An Introduction to Their Design, Performance, and Selection. Wiley.
HAMADI, L., MANSOURI, S., OULMI, K. & KARECHE, A. 2018. The use of amino acids as corrosion inhibitors for metals: A review. *Egyptian journal of petroleum,* 27(4)**,** 1157-1165.
LAWES, S., HAINSWORTH, S., BLAKE, P., RYDER, K. & ABBOTT, A. 2010. Lubrication of steel/steel contacts by choline chloride ionic liquids. *Tribology letters,* 37(2)**,** 103-110.
LI, Y., LI, H., FAN, X., CAI, M., XU, X. & ZHU, M. 2022. Green and economical bet-based natural deep eutectic solvents: a novel high-performance lubricant. *ACS Sustainable Chemistry & Engineering,* 10(22)**,** 7253-7264.
LI, Y., LI, Y., LI, H., FAN, X., YAN, H., CAI, M., XU, X. & ZHU, M. 2023. Insights into the tribological behavior of choline chloride—Urea and choline chloride—Thiourea deep eutectic solvents. *Friction,* 11(1)**,** 76-92.
LIU, M., NI, J., ZHANG, C., WANG, R., CHENG, Q., LIANG, W. & LIU, Z. 2024. The application of ionic liquids in the lubrication field: their design, mechanisms, and behaviors. *Lubricants,* 12(1)**,** 24.
LIU, X. & LIU, Z. 2010. Research progress on flash point prediction. *Journal of Chemical Engineering Data,* 55(9)**,** 2943-2950.
MORAIS, A. R. C., SIMONI, L. D., SHIFLETT, M. B., SCURTO, A. M. & DATA, E. 2020. Viscosity and density of a polyol ester lubricating oil saturated with compressed hydrofluoroolefin refrigerants. *Journal of Chemical,* 65(9)**,** 4335-4346.
NGUYEN, D. T., JOHIR, M. A. H., MAHLIA, T. I., SILITONGA, A., ZHANG, X., LIU, Q. & NGHIEM, L. D. 2024. Microalgae-derived biolubricants: Challenges and opportunities. *Science of the Total Environment,* 954(176759.
QADER, I. B. 2021. Enhance dissolution rate and solubility of solid drugs through pharmaceutical deep eutectic solvents. *Zanco Journal of Pure and Applied Sciences,* 33(3)**,** 98-106.
QADER, I. B., GANJO, A. R., AHMAD, H. O., QADER, H. A. & HAMADAMEEN, H. A. 2024. Antibacterial and antioxidant study of new pharmaceutical formulation of didecyldimethylammonium bromide via pharmaceutical deep eutectic solvents (PDESs) principle. *AAPS PharmSciTech,* 25(1)**,** 25.
RAHMALIA, W., SHOFIYANI, A., SUTIKNYAWATI, Y. & SEPTIANI, S. 2022. Simple green routes for metal-bixin complexes synthesis using glycerol-based deep eutectic solvent. *Indonesian Journal of Chemistry,* 22(6)**,** 1759-1767.
SAD, C. M., LACERDA JR, V., FILGUEIRAS, P. R., RIGONI, V. S., BASSANE, J. O. F., CASTRO, E. Q. V., PEREIRA, K. T. S., SANTOS, M. F. & FUELS 2014. Limitations of the pour point measurement and the influence of the oil composition on its detection using principal component analysis. *Energy,* 28(3)**,** 1686-1691.
SALTYKOV, S., MAKAROV, G., TOROPTSEVA, E. & FILATOVA, Y. B. 2004. Anodic behavior of white iron phases in oxalic media. *Protection of Metals,* 40(56-61.
SCHNEIDER, M. P. 2006. Plant-oil-based lubricants and hydraulic fluids. *Journal of the Science of Food and Agriculture,* 86(12)**,** 1769-1780.
SCHULER, E., GROOTEN, L., KASIREDDY, M., MORE, S., SHIJU, N. R., TANIELYAN, S. K., AUGUSTINE, R. L. & GRUTER, G.-J. M. 2023. Oxalic acid hydrogenation to glycolic acid: heterogeneous catalysts screening. *Green Chemistry,* 25(6)**,** 2409-2426.
SERNAGLIA, M., BARTOLOME, M., VIESCA, J., GONZáLEZ, R. & BATTEZ, A. H. 2025. Application of deep eutectic solvents in lubrication: A review. *Journal of Molecular Liquids,* 127464.
SERNAGLIA, M., RIVERA, N., BARTOLOME, M., FERNáNDEZ-GONZáLEZ, A., GONZáLEZ, R. & VIESCA, J. 2024. Tribological behavior of two novel choline acetate-based deep eutectic solvents. *Journal of Molecular Liquids,* 414(126102.
SHAH, R., WOYDT, M. & ZHANG, S. 2021. The economic and environmental significance of sustainable lubricants. *Lubricants,* 9(2)**,** 21.
SHAHBAZ, K., MJALLI, F., HASHIM, M. A. & ALNASHEF, I. 2011. Prediction of deep eutectic solvents densities at different temperatures. *Thermochimica acta,* 515(1-2)**,** 67-72.
SMITH, E. L., ABBOTT, A. P. & RYDER, K. S. 2014. Deep eutectic solvents (DESs) and their applications. *Chemical reviews,* 114(21)**,** 11060-11082.
SOKOLNIKOV, A., BEZBORODOV, Y. N. & SHRAM, V. 2016. Apparatus for Determining of the Pour Point of Crude Oil and Petroleum Products. *Procedia Engineering,* 150(486-489.
SONI, S., AGARWAL, M. & REVIEWS 2014. Lubricants from renewable energy sources – a review. *Green Chemistry Letters,* 7(4)**,** 359-382.
TANG, Z., LI, S. & SCIENCE, M. 2014. A review of recent developments of friction modifiers for liquid lubricants (2007–present). *Current opinion in solid state,* 18(3)**,** 119-139.
TRETHEWEY, K. R. & CHAMBERLAIN, J. 1995. *Corrosion for Science and Engineering*, Longman
VIEIRA, L., SCHENNACH, R. & GOLLAS, B. 2015. In situ PM-IRRAS of a glassy carbon electrode/deep eutectic

solvent interface. *Physical Chemistry Chemical Physics,* 17(19)**,** 12870-12880.
WANG, H., LIU, S., ZHAO, Y., WANG, J. & YU, Z. 2019. Insights into the hydrogen bond interactions in deep eutectic solvents composed of choline chloride and polyols. *ACS Sustainable Chemistry & Engineering,* 7(8)**,** 7760-7767.
ZHANG, H., CHEN, Y., CHU, A., HU, H. & ZHAO, Y. 2023. Synthesis of Imidazole-Based Deep Eutectic Solvents as Solid Lubricants: Lubricated State Transition. *Materials,* 16(19)**,** 6579.
ZHANG, Q., VIGIER, K. D. O., ROYER, S. & JEROME, F. 2012. Deep eutectic solvents: syntheses, properties and applications. *Chemical Society Reviews,* 41(21)**,** 7108-7146.
ZHANG, Y., HAN, J. & LIAO, C. 2016. Insights into the properties of deep eutectic solvent based on reline for Ga-controllable CIGS solar cell in one-step electrodeposition. *Journal of The Electrochemical Society,* 163(13)**,** D689.